

sponds to a dipole moment of 1.4×10^{-15} cm times e . This upper bound on the electric dipole moment of the electron is three times lower than the bound set by Nelson *et al.*,⁵⁴ but not as good as the bound of 4×10^{-16} cm times e set by Wilkinson *et al.*⁵⁵ or the bound of 10^{-15} set by Goldemberg and Torizuka.⁵⁶

In view of the molecular orbital theory of crystal fields developed previously, one may question the use of the simple electrostatic crystal field theory in calculating the dipole effect. Unfortunately, while the semiempirical molecular orbital theory is very good in treating the chrome-ligand interactions, it is unsatisfactory in treating the interactions between the various elec-

tron orbitals on the chromium ion, and it is just these interactions which are dominant in calculating the dipole effect. The electrostatic model used in evaluating Eq. (20) is probably conservative in estimating the value of $\nabla\phi^u$.

The experimental limitations which prevented a better upper bound from being set on the electric dipole moment of the electron by this method arise mainly from instrumental instabilities over the period of a run. More fundamental, however, is the limitation that this measurement depends on the calculation of effective crystalline fields in a solid, a problem whose solution is still beset with considerable uncertainty. The approximations used in the calculations here are quite crude, but a better calculation must await better wave functions and energy levels for excited states of an atom in a solid, and a better theory of the crystalline field.

⁵⁴ D. F. Nelson, A. A. Schupp, R. W. Pidd, and H. R. Crane, *Phys. Rev. Letters* **2**, 492 (1959).

⁵⁵ D. T. Wilkinson and H. R. Crane, *Phys. Rev.* **130**, 852 (1963).

⁵⁶ J. Goldemberg and Y. Torizuka, *Phys. Rev.* **129**, 2580 (1963).

Theory of the Magnetic and Optical Properties of Cr_2O_3 †

G. W. PRATT, JR., AND P. T. BAILEY

Materials Theory Group, Department of Electrical Engineering, Massachusetts Institute of Technology, Cambridge, Massachusetts

(Received 18 April 1963)

Cr_2O_3 is discussed from the point of view of pairs of Cr ions with strong exchange coupling between members of the pair and subjected to a relatively weak molecular field. This is done using the Oguchi method. The anomalous behavior of the parallel susceptibility above T_N and low-temperature spin-saturation value are explained. If the spin system is assumed to be canted, it is possible to explain the nonzero value of χ_{\parallel} at 0°K and the resultant optical properties are found to be in good agreement with experiment.

I. INTRODUCTION

THIS study of the magnetic and optical properties of Cr_2O_3 was stimulated by the very interesting high-resolution measurements of the optical absorption of Cr_2O_3 at 4.2°K by Wickersheim.¹ He found that using a spin-Hamiltonian description of an individual Cr^{3+} ion subjected to both a crystal field and an effective magnetic field due to exchange, there appear various discrepancies between the consequences of this model and the experimental results. Since Cr_2O_3 can be thought of as being constructed from a set of parallel chains of atoms with each chain a c axis along which the Cr^{3+} ions are grouped as pairs of Cr^{3+} ions with a relatively large separation between pairs, it seems more natural to use a model which treats the optical properties of a pair of Cr^{3+} ions rather than individual Cr^{3+} ions. In Fig. 1 we show the atomic arrangement along the c axis. Our model consists, then, of a pair of Cr^{3+} ions such as the pair $A-B$ in Fig. 1 with an antiferromagnetic superex-

change coupling between these ions. The crystalline environment subjects the pair to a crystal field and an effective magnetic field from exchange interactions with the pair. With this geometric arrangement, the method of Oguchi² seems ideal to discuss Cr_2O_3 and this is the scheme used in this analysis.

The results obtained are very satisfactory. Not only can the optical properties be accounted for but the anomalous magnetic properties of Cr_2O_3 can also be explained by the same model. These anomalies are the failure of the parallel magnetic susceptibility χ_{\parallel} to vanish at 0°K and the failure of χ_{\parallel} to drop sharply as the temperature increases through the Néel point. Our theory further predicts that the sublattice spin per Cr will not saturate at 0°K to 1.5 but more nearly to 1.3. In addition, we predict that the Cr spins order in some form of canted spins forming spirals. The introduction of canted spins into our model provides an explanation of the low-temperature behavior of χ_{\parallel} and at the same time improves agreement with the optical anisotropy

† This work was supported in part by the U. S. Office of Naval Research.

¹ K. A. Wickersheim, *J. Appl. Phys.* **34**, 1224 (1963).

² T. Oguchi, *Progr. Theoret. Phys. (Kyoto)* **13**, 148 (1955).

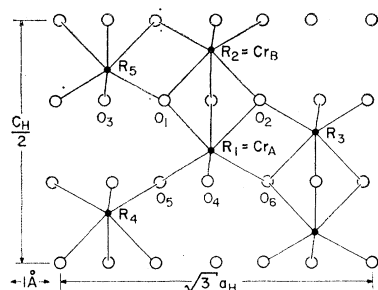


FIG. 1. Projection of Cr_2O_3 on $(\bar{1}10)$. Cr ions at R_1 and R_2 lie along the c axis and form the Oguchi pair. The authors are indebted to Professor R. Newnham for this figure [R. E. Newnham and Y. M. de Haan, *Z. Krist.* **117**, 235 (1962)].

experiments. These results and predictions are explained in detail in the body of the paper.

Section II of the paper treats the pair of Cr^{3+} ions by the Oguchi method and the sublattice magnetization is determined self-consistently as a function of the magnitude and direction of the molecular field at each member of the Cr—Cr pair. Besides finding the eigenstates and energy spectrum for the pair when both spins are $\frac{3}{2}$, these properties are also determined when one of the Cr^{3+} ions is excited to a doublet ($S=\frac{1}{2}$) state. χ_{11} is also evaluated. In Sec. III the results concerning the magnetic properties are discussed. Section IV treats the optical properties of the pair using the theory of Sugano and Tanabe³ for the Zeeman effect in ruby. Our main results are summarized in Sec. V.

II. SUBLATTICE MAGNETIZATION AND PARALLEL SUSCEPTIBILITY

The method used to find the sublattice magnetization and parallel susceptibility is that due to Oguchi. In the ordinary molecular field approach one considers a single magnetic ion and replaces the exchange or superexchange interactions that it has with neighboring ions by static magnetic or so-called molecular fields. Oguchi's method goes a step beyond this and considers a pair of magnetic atoms with the actual exchange interaction between them fully included so that mutual spin fluctuations are allowed but the exchange interactions with ions exterior to the pair are again replaced by static molecular fields proportional to the average spin of one of the members of the pair. The average value of the spin at a given temperature is found by a self-consistent condition. Since the crystal structure of Cr_2O_3 emphasizes pairs of Cr^{3+} ions, the Oguchi method should be a marked improvement over the molecular field model.

The Hamiltonian used to describe the pair of exchange-coupled Cr^{3+} ions is

$$\mathcal{H} = 2J_{AB}\mathbf{S}_A \cdot \mathbf{S}_B - Y\langle S_{AZ} \rangle (S_{AZ} - S_{BZ}) + B\langle S_{AZ} \rangle (S^+ + S^-) + D(S_{AZ}^2 + S_{BZ}^2) - g\mu_0 H S_z. \quad (1)$$

The first term in (1) is the superexchange coupling of a pair of nearest neighbor Cr^{3+} ions on the c axis. From the

work of Statz, Weber, Rimai, DeMars, and Koster⁴ on ruby it is known that this exchange coupling dominates all others by perhaps as much as an order of magnitude. It is estimated by Statz *et al.* in ruby to be 350 cm^{-1} and by Wickersheim¹ at about 250 cm^{-1} for Cr_2O_3 .

The second term describes the coupling of the spins of the Cr—Cr pair to the z component of the molecular field arising from the environment. This z component of the field, of magnitude $Y\langle S_{AZ} \rangle / g\mu_B$, is positive at the A site and negative at the B site and assumed proportional to the thermal average of the z component of S_{AZ} . The parameter Y is ordinarily proportional to the number of neighbors setting up the molecular field and to the strength of the exchange coupling to these neighbors. In Cr_2O_3 the situation is not so simple and this is an essential feature contributing to the atypical results obtained. It can be seen from Fig. 1 that each of the Cr—Cr pair is directly coupled to two separate groups of three oxygen ions. These groups each form a plane perpendicular to the c axis and the Cr ion associated with the planes lies between them. Each oxygen ion is in turn coupled to three other Cr^{3+} ions by unequal exchange forces whose values are less than the principal exchange J_{AB} and otherwise unknown. We do know that the strength of the z component of the molecular field will be proportional to $\langle S_{AZ} \rangle$ and the constant of proportionality Y is regarded as a parameter. It will be determined by finding the behavior of the model for several values of Y and comparing the results with experiment. It will be seen that too large a value of Y leads to a ridiculously high Néel point while too small a value leads to an unreasonably low-sublattice spin saturation value at 0°K .

The third term of (1) allows for the molecular field at the A and B sites to have an x component. For small values of the x component there is almost no effect on the Néel point or on the sublattice saturation value. However, the 0°K limit of χ_{11} is very sensitive to B in (1) and the optical anisotropy is strongly affected by it.

The fourth term in (1) represents the uniaxial anisotropy. It was included in the computer program for generality but for Cr_2O_3 the zero-field splitting constant is very small according to Foner⁵ and we will neglect this term.

Finally, the fifth term in (1) describes the effect of an external magnetic field applied in the z direction, i.e., along the c axis. This was included so that χ_{11} could be evaluated. Since we are interested only in the limit of vanishing applied field, this term need not be carried along in the calculation as will be seen.

The eigenstates and energies of the Hamiltonian (1) were found for two physical situations. First, the normal case in which both Cr^{3+} ions have spin $S=\frac{3}{2}$ was studied. Second, the eigenproperties were found when one of the

⁴ H. Statz, M. Weber, L. Rimai, G. DeMars, and G. Koster, *J. Phys. Soc. Japan* **17**, Suppl. B1, 428 (1962).

⁵ S. Foner, *Phys. Rev.* **130**, 183 (1963).

³ S. Sugano and Y. Tanabe, *J. Phys. Soc. Japan* **13**, 880 (1958).

Cr³⁺ ions had been optically excited to the $S=\frac{1}{2}$ state. We first discuss the normal configuration.

A pair of Cr ions each having a spin $S=\frac{3}{2}$ leads to 16 states for the pair and the 16×16 energy matrix was set up using the representation $|S_T, M_T\rangle$ in which $S_T=S_A+S_B$ and $M_T=M_{S_A}+M_{S_B}$ are good quantum numbers. The matrix elements for a fixed choice of Y and B depend on the thermal average $\langle S_{AZ} \rangle$ which is unknown. This quantity is determined self-consistently at each temperature by assuming an initial value for $\langle S_{AZ} \rangle$, finding the eigenstates $|i\rangle$ and energies E_i of the pair, and using these results to calculate $\langle S_{AZ} \rangle$ from

$$\langle S_{AZ} \rangle = \frac{\sum_{i=1}^{16} \langle i | e^{-\beta E_i} S_{AZ} | i \rangle}{\sum_{i=1}^{16} \langle i | e^{-\beta E_i} | i \rangle}. \quad (2)$$

If the initial and calculated values of $\langle S_{AZ} \rangle$ differed by more than 0.001, a new guess of $\langle S_{AZ} \rangle$ was made and the process repeated until this agreement was obtained. This procedure was carried out starting at low temperatures and continuing to the point where $\langle S_{AZ} \rangle$ vanishes, which we identify with the Néel temperature. Both T_N and the sublattice magnetization as a function of temperature were found for a series of choices for Y and B . At the same time we can find χ_{11} as follows. The thermal average of the z component of the magnetization in the presence of a small field in that direction is

$$\langle M_Z \rangle = \frac{g\mu_B}{Z} \sum_i \langle i | \exp[-\beta \mathcal{H}_0] \left\{ 1 - \int_0^1 d\lambda \exp[\lambda \beta \mathcal{H}_0] \right. \\ \left. \times \beta g\mu_B H S_Z \exp[-\beta \lambda \mathcal{H}_0] + \dots \right\} S_Z | i \rangle, \quad (3)$$

where \mathcal{H}_0 is the Hamiltonian (1) with the external magnetic field set equal to zero and Z is the partition function. Because of the x component of the molecular field, S_Z does not commute with \mathcal{H}_0 and we find

$$\chi_{11} = - \frac{\partial \langle M_Z \rangle}{\partial H} \Big|_{H=0} \\ = \frac{\beta g^2 \mu_B^2}{Z} \sum_i \langle i | \exp[-\beta \mathcal{H}_0] \int_0^1 d\lambda S_Z(\lambda) S_Z | i \rangle, \quad (4)$$

where

$$S_Z(\lambda) = \exp[\lambda \beta \mathcal{H}_0] S_Z \exp[-\lambda \beta \mathcal{H}_0]. \quad (5)$$

Having found the properties of the normal configuration of the pair, the eigenstates and energies were found with one of the Cr ions excited to the $S=\frac{1}{2}$ state. The secular equation is now 8×8 and the excited pair was described by the Hamiltonian given in (1). Of course, we should allow for a change in J_{AB} , Y , and B for the excited system. However, the qualitative features we hope to explain are not seriously affected by the omission of these refinements.

III. RESULTS CONCERNING THE MAGNETIC PROPERTIES

In Fig. 2 the sublattice magnetization and χ_{11} are given as a function of temperature. These results are all

for the molecular field entirely along the c axis (z axis), hence, with B of (1) set equal to zero. The four separate magnitudes of the molecular field are specified by the Y values. As mentioned above, the running parameter in the calculation is $w=\beta J$ and this has been converted to a temperature scale by assuming $J=250 \text{ cm}^{-1}$. It is to be emphasized that the Oguchi theory is not accurate enough to determine a value of J from the Néel temperature that is consistent with independent, e.g., optical determinations of the exchange strength. Thus, the temperature scale is somewhat arbitrary. Furthermore, we have no experimental values for the coupling of the Cr_A—Cr_B pair to its surroundings. Therefore, the results obtained are clearly of a qualitative nature.

A number of important features are apparent at once from a study of Fig. 2. First, the z -component sublattice spin per ion does not saturate to $\langle S_{AZ} \rangle = \frac{3}{2}$ at 0°K for the range of Y values considered. The reason for this is quite simple. As noted $B=0$ here and if Y were also zero, then the system would reduce to a collection of isolated Cr—Cr pairs. In this limit $\langle S_{AZ} \rangle$ at 0°K would vanish altogether. As Y increases from zero, the saturation value of $\langle S_{AZ} \rangle$ rises sharply but not discontinuously as shown in Fig. 3. For a simple cubic lattice of spins of $\frac{3}{2}$ the value of Y is 10 in units of J and saturation is achieved. Increasing Y so as to obtain spin saturation of $\langle S_{AZ} \rangle = \frac{3}{2}$ at 0°K rapidly raises the Néel temperature as shown in Fig. 4 and the Oguchi description would lead to a ridiculously high Néel point. Even for $Y=1.8$ which gives $\langle S_{AZ} \rangle \cong 1.4$ at 0°K, the corresponding T_N is over 2000°K as compared to the experimental value of 308°K. Oguchi's scheme will give too high a Néel point if the correct values of the exchange couplings are used. This is characteristic of such theories. However, the result should be correct to within a factor of two or three. On this basis it seems quite reasonable to predict $\langle S_{AZ} \rangle$ to be about 1.3 at 0°K.

The second striking feature of Fig. 2 is the behavior of χ_{11} just above T_N . Instead of dropping sharply for $T > T_N$, χ_{11} is seen to continue to increase. This is

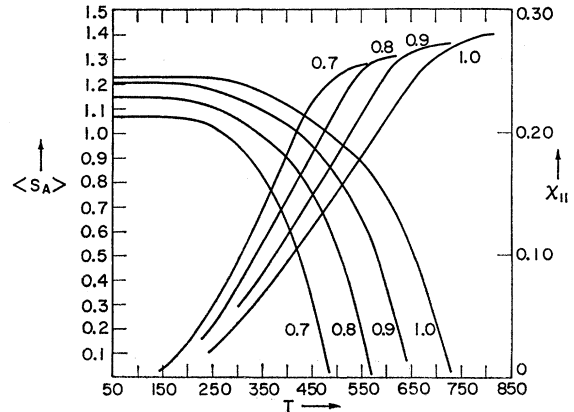


Fig. 2. Sublattice spin per ion $\langle S_A \rangle$ and the parallel susceptibility χ_{11} as a function of temperature for various molecular field strengths given by $Y=0.7$ to 1.0.

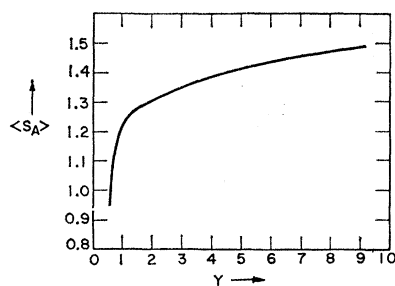


FIG. 3. Saturation at 0°K of the sublattice spin per ion ($\langle S_A \rangle$) as a function of the strength of the molecular field exerted on the pair.

another consequence of the crystal structure and of the fact that above T_N our model reduces to a collection of uncorrelated Cr—Cr pairs with strong coupling within each pair. This anomalous behavior of χ_{11} is in complete accord with the recent measurements by Foner on single-crystal material as shown in Fig. 5.

The third feature of Fig. 2 requiring comment is the result that at 0°K χ_{11} will vanish independent of the choice of Y as long as B is zero. According to Foner's measurements, χ_{11} does not vanish. Therefore, in order to obtain a nonzero χ_{11} at 0°K, the molecular field was given an x component at each Cr ion of the Cr_A — Cr_B pair of magnitude $B\langle S_{Az} \rangle / 2g\mu_B$. From (4) we obtain

$$\chi_{11} = \frac{g^2\mu_B^2}{Z} \sum_{i=1}^{16} \beta \exp[-\beta E_i] \langle i | S_z | i \rangle^2 + \frac{g^2\mu_B^2}{Z} \sum_{i \neq j} \frac{e^{-\beta E_i}}{(E_i - E_j)} \{ \exp[\beta(E_i - E_j)] - 1 \} \times \langle i | S_z | j \rangle \langle j | S_z | i \rangle. \quad (6)$$

The second term on the right of (6) is that due to the x component of the molecular field and which remains nonzero in the 0°K limit.

Figure 6 shows the effect of including an x component of the molecular field. It completely controls the low-temperature behavior of χ_{11} but does not materially affect $\langle S_{Az} \rangle$ at 0°K, nor the value of T_N , nor the behavior of χ near T_N . In effect we can then determine the value of B by requiring that the ratio $\chi_{11}(T_N)/\chi_{11}(0^\circ\text{K})$ calculated be equal to the experimental value determined by Foner. The dependence of this ratio on B is shown in Fig. 7. He found on different samples that the ratio varied from 12.5 to 20. The range of B found in this manner is $0.3 \leq B \leq 0.38$ and this corresponds to an

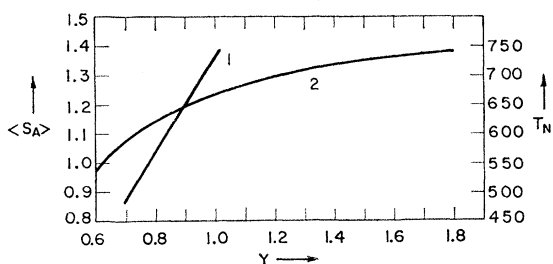


FIG. 4. Curve 1 shows the dependence of the Néel temperature on the strength of the molecular field and curve 2 gives $\langle S_A \rangle$ as a function of Y .

angular variation of $31 \leq \theta \leq 37$ deg between the molecular field and the R_1 — R_2 axis as shown in Fig. 8. Of course, this would mean that the Cr_A — Cr_B pair would have a net magnetic moment in the x direction. Since no net moment is observed for the Cr_2O_3 crystal, some cancelling process such as spiraling of the net molecular field per pair along the R_1 — R_2 axis would have to occur. Because the Oguchi method looks only at a pair of Cr ions subjected to an averaged environment we are unable to make a more precise statement on the spin orientation of the crystal.

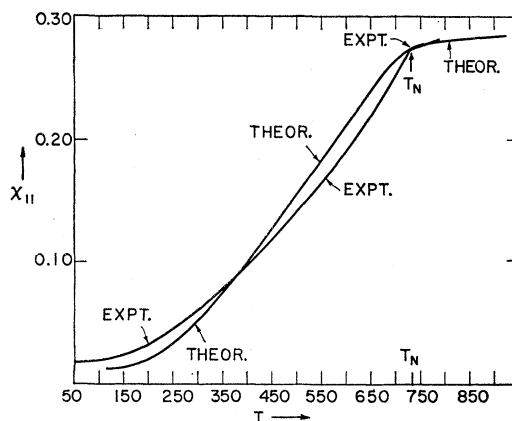


FIG. 5. Comparison of Foner's experimental results (Ref. 5) with theory. Foner's temperature scale was fitted to that used in this work and the values of χ_{11} at T_N were made equal.

IV. OPTICAL PROPERTIES OF Cr_2O_3

As remarked in the previous section, the 16×16 secular equation for the Cr_A — Cr_B pair is solved for both the energy spectrum and the eigenstates. This is also done when one of the Cr ions is excited to the $S = \frac{1}{2}$, 2E state. Under the influence of the trigonal part of the crystal field and the spin orbit interaction the 2E state of the optically excited Cr-ion splits into an \bar{E} level and a ${}^2\bar{A}$ level. Thus, there are 8 excited pair states of the form $\text{Cr}_A({}^2\bar{E})$ — $\text{Cr}_B({}^4A_2)$ and 8 of the form $\text{Cr}_A({}^2\bar{A})$ — $\text{Cr}_B({}^4A_2)$. In Fig. 9 the levels for the canted and uncanted cases are shown. Only the first three of the 16 levels of the $\text{Cr}_A({}^4A_2)$ — $\text{Cr}_B({}^4A_2)$ pair are represented and in this figure the 2E splitting of the excited Cr is neglected. All energies are in units of the Cr_A — Cr_B exchange energy J . The energy separation between the ground and first excited state of the normal pair is approximately $3J$ so that at low temperatures the initial state of the optical transition is always the ground state. The only excited states that need be considered as being final states in the optical transitions from the ground state are the lowest two of the 8 excited pair states of each symmetry, i.e., $(\bar{E}^2 - {}^4A_2)$ and $({}^2\bar{A} - {}^4A_2)$. This is because the theoretical transition probabilities to the upper excited states are very small. Moreover, these upper states are sufficiently high in energy so that they are out of the energy range in which Wickersheim obtained his high-resolution results.

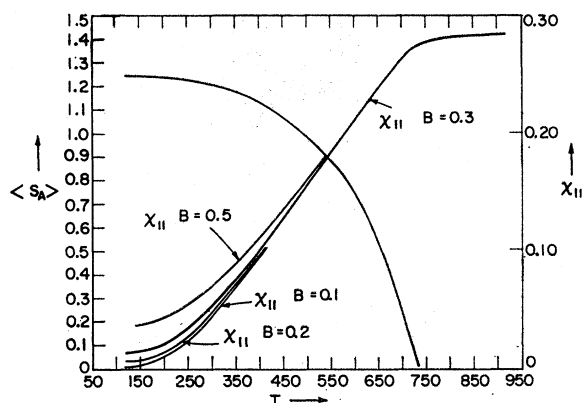


FIG. 6. Dependence of X_{II} on the angle $\theta = \tan^{-1}(2B/Y)$ between the molecular field and the c axis (see Fig. 8) for $Y=1.0$.

For the purposes of computing the optical transition probabilities it is convenient to express the pair states as linear combinations of products of Cr single ion states. This is done for the canted and uncanted cases in Appendix I for the ground state and excited states of interest. The optical-transition probabilities can now be directly found from the results of Sugano and Tanabe's work on ruby. The results are shown in Fig. 10 where they are contrasted with the single ion, molecular-field model.

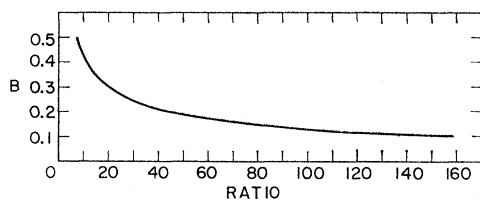


FIG. 7. Ratio of $X_{II}(T_N)/X_{II}(0^\circ\text{K})$ as a function of the angle $\theta = \tan^{-1}2B/Y$ between the molecular field and the c axis.

It is seen in Fig. 10 that the transition from the ground state to the lowest $\text{Cr}_A(^2\bar{E})-\text{Cr}_B(^4A_2)$ state is purely of σ character, i.e., seen only if the electric field of the incident light is perpendicular to the c axis; while the transition to the lowest $\text{Cr}_A(^2\bar{A})-\text{Cr}_B(^4A_2)$ state is purely of π character requiring the electric field to be parallel to the c axis. The single-ion molecular-field model exhibits the same kind of optical anisotropy. An important difference between the two models lies in the fact that transitions from the ground state to higher excited states in the single ion, molecular field model are strictly forbidden because a ΔM_s of ± 2 is involved. These transitions are not forbidden in the Oguchi pair approach and they are allowed by virtue of the exchange

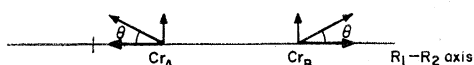


FIG. 8. Proposed molecular field configuration for a single pair. The net molecular field component perpendicular to the c axis is expected to spiral about the c axis as one moves along it so that there will be no net moment.

interaction $J_{AB}\mathbf{S}_A \cdot \mathbf{S}_B$ which is correctly included in this scheme. This exchange coupling is the dominating factor in determining the actual form of the various states shown in Table I. Although the single ion model could be extended by using the generalized spin Hamiltonian of Koster and Statz⁶ to include a cubic term in

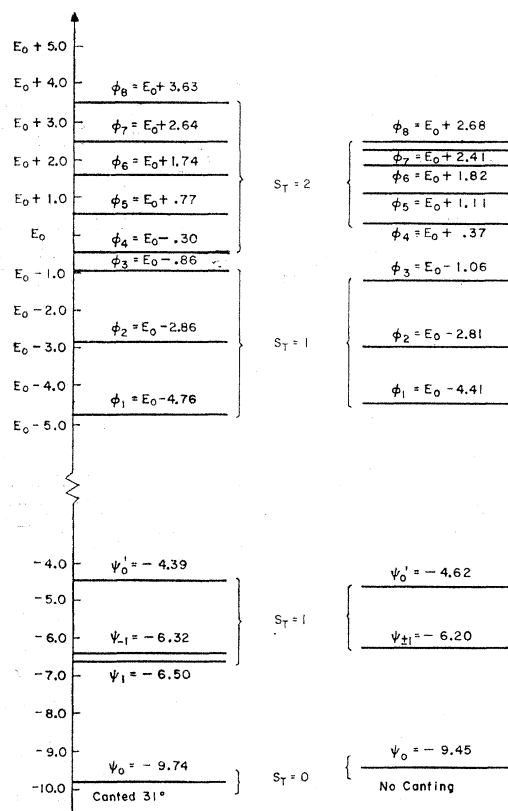


FIG. 9. Energy levels for the pair in a canted ($\theta=31^\circ$) and uncanted molecular field. The total pair spin S_T is diagonal in the uncanted case and ground configuration levels are shown only for $S_T=0$ and $S_T=1$ since those for $S_T=2$ and 3 are higher lying and of no interest. All eight excited states, constructed from an $S=\frac{3}{2}$ Cr ion and an $S=\frac{3}{2}$ Cr ion pair, are shown.

the Cr spin, this would mask the simple physical basis by which the single ion "forbidden" transitions indicated in Fig. 10 become permissible. Wickersheim's experimental results are given in Fig. 11 showing the four observed absorptions and the optical anisotropy.

Not only does the pair approach permit the extra transitions, but it can be used to study the optical anisotropy and its relation to the spin structure. If no canting is allowed, the transitions from the ground state to the excited states $\varphi_2(\bar{E}-^4A_2)$ and $\varphi_2'(\bar{A}-^4A_2)$ are both of pure σ character. This is not in agreement with experiment as can be seen from Fig. 11 where transition III is mainly of π character and IV of σ character. For the canted system, $\theta=31^\circ$, we see from Fig. 10 that the transition to φ_2 which should correspond to IV of Fig. 11 remains pure σ but that to φ_2' which should

⁶ G. Koster and H. Statz, Phys. Rev. **113**, 445 (1959).

correspond to III is now no longer pure σ but predominantly π . Wickersheim's results appear to show that III has very little σ character, apparently less than our pair model shows. We feel that our theoretical results on the polarization provide some support for a canted spin model but obviously do not provide a conclusive argument.

V. DISCUSSION

Our application of the Oguchi pair approximation method has resulted in a qualitatively satisfactory description of several anomalous properties of Cr_2O_3 . The failure of the sublattice spin per ion to saturate at 1.5 at 0°K and the behavior of χ_{11} for $T > T_N$ are direct consequences of the pair which has a strong internal exchange coupling but which experiences a relatively weak molecular field because of the structure of Cr_2O_3 . The results are qualitative in that the exchange couplings have to be regarded as disposable parameters. If we examine the numerical value of χ_{11} at T_N as a function of Y and $W_N^{-1} = kT_N/J_{AB}$ as a function of Y , it is found that both quantities depend linearly on Y . A value of $J_{AB} = 140 \text{ cm}^{-1}$ and Y of 0.81 with $B = 0.3$ leads to $T_N = 308^\circ\text{K}$ and equality of the theoretical and experimental values of χ_{11} at T_N of $26 \times 10^{-6} \text{ emu/g}$. However, this fit made at T_N leads to $\langle S_{AZ} \rangle$ at 0°K of 1.15 which seems rather low.

The model also can account for the nonzero value of χ_{11} at 0°K and gives a reasonable description of the optical anisotropy if the molecular field is canted as shown in Fig. 8. The angle between the molecular field and the c axis which is required for the theory to yield the values of χ_{11} at 0°K measured by Foner is approximately 30° . This seems like a very large angle and there may well be other contributing factors to Foner's re-

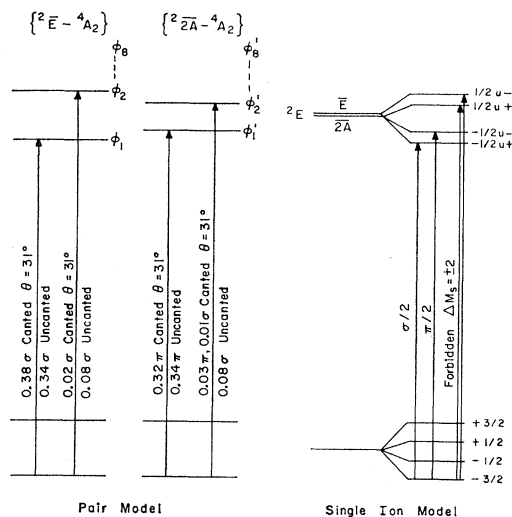


FIG. 10. Optical transitions for the pair and single ion models with intensities and polarizations indicated.

⁷ R. Orbach [Phys. Rev. **115**, 1189 (1959)] has considered the resonance properties of a spin system of the form shown in Fig. 8. He points out that χ_{11} is nonzero at 0°K for a canted system.

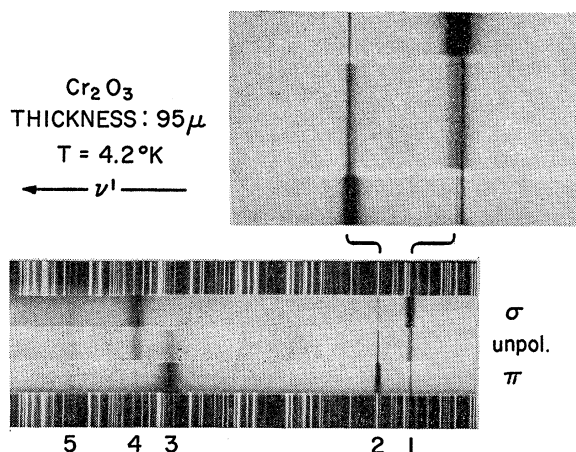


FIG. 11. The authors are indebted to K. Wickersheim for permission to reproduce his experimental results for Cr_2O_3 . Lines 1, 2, 3, and 4 occurred at approximately 13 743, 13 764, 13 903, and $13\,926 \text{ cm}^{-1}$, respectively.

sults. Some type of spiral structure must be invoked so that no net moment arises in the canted model. At this time the neutron diffraction study of Cr_2O_3 is not complete so that our results cannot appeal to these data for support. The best that can be said is that preliminary results do not rule out our canted spiral description. It would be interesting if a theoretical description of magnetic and optical properties could also partially establish the magnetic ordering.

APPENDIX I. GROUND STATES AND EXCITED STATES FOR AN UNCANTED AND CANTED PAIR OF Cr IONS IN Cr_2O_3

Ground state of the $\text{Cr}(^4A_2) - \text{Cr}(^4A_2)$ pair expressed as a linear combination of products of single ion states. We use the notation $|M_s, M_{s'}\rangle$ to denote $|\text{Cr}(^4A_2, M_s)\text{Cr}(^4A_2, M_{s'})\rangle$.

Uncanted pair $\theta = 0^\circ$,

$$\psi_0 = 0.873 \left| \frac{3}{2}, -\frac{3}{2} \right\rangle - 0.448 \left| \frac{1}{2}, -\frac{1}{2} \right\rangle + 0.182 \left| -\frac{1}{2}, \frac{1}{2} \right\rangle - 0.073 \left| -\frac{3}{2}, \frac{3}{2} \right\rangle.$$

Canted pair $\theta = 31^\circ$,

$$\psi_0 = -0.886 \left| \frac{3}{2}, -\frac{3}{2} \right\rangle + 0.418 \left| \frac{1}{2}, \frac{1}{2} \right\rangle - 0.146 \left| -\frac{1}{2}, \frac{1}{2} \right\rangle + 0.066 \left| -\frac{3}{2}, \frac{3}{2} \right\rangle.$$

First and second states ϕ_1 and ϕ_2 of the excited pair $\text{Cr}(^2E\bar{E} \text{ or } ^2\bar{2}\bar{A}) - \text{Cr}(^4A_2)$ expressed as linear combinations of products of single ion states.

Uncanted pair $\theta = 0^\circ$,

$$\phi_1 = 0.946 \left| \frac{1}{2}, -\frac{3}{2} \right\rangle - 0.331 \left| -\frac{1}{2}, -\frac{1}{2} \right\rangle, \\ \phi_2 = 0.868 \left| \frac{1}{2}, -\frac{1}{2} \right\rangle - 0.500 \left| -\frac{1}{2}, \frac{1}{2} \right\rangle.$$

Canted pair $\theta = 31^\circ$,

$$\phi_1 = 0.908 \left| \frac{1}{2}, -\frac{3}{2} \right\rangle - 0.196 \left| \frac{1}{2}, -\frac{1}{2} \right\rangle - 0.299 \left| -\frac{1}{2}, -\frac{1}{2} \right\rangle + 0.196 \left| -\frac{1}{2}, \frac{1}{2} \right\rangle, \\ \phi_2 = 0.252 \left| \frac{1}{2}, -\frac{3}{2} \right\rangle + 0.807 \left| \frac{1}{2}, -\frac{1}{2} \right\rangle + 0.146 \left| -\frac{1}{2}, -\frac{1}{2} \right\rangle - 0.429 \left| -\frac{1}{2}, \frac{1}{2} \right\rangle - 0.233 \left| \frac{1}{2}, \frac{1}{2} \right\rangle + 0.170 \left| -\frac{1}{2}, \frac{3}{2} \right\rangle.$$

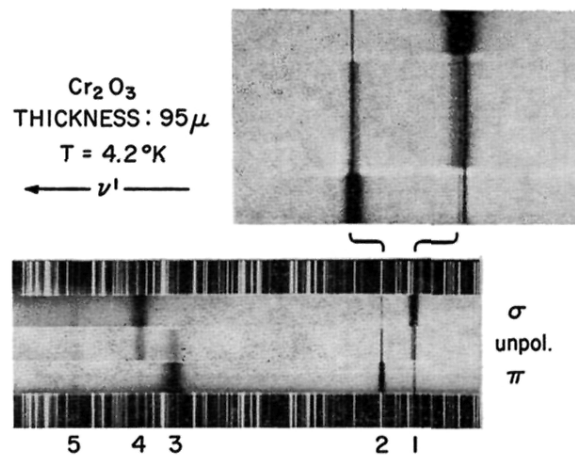


FIG. 11. The authors are indebted to K. Wickersheim for permission to reproduce his experimental results for Cr_2O_3 . Lines 1, 2, 3, and 4 occurred at approximately $13\,743$, $13\,764$, $13\,903$, and $13\,926\text{ cm}^{-1}$, respectively.